

## Supporting information

### Mechanical properties soft hydrogels: assessment by scanning ion-conductance microscopy and atomic force microscopy

Tatiana N. Tikhonova, Yuri M. Efremov, Vasilii S. Kolmogorov, Aleksei P. Iakovlev, Nikolay N. Sysoev, Peter S. Timashev, Victor V. Fadeev, Alexander S. Tivtikyan, Sergey V. Salikhov, Petr V. Gorelkin, Yuri E. Korchev, Alexander S. Erofeev, Evgeny A. Shirshin

Table S1. The parameters of SICM and AFM experiments

	Young's modulus $E$ determination using intrinsic force (colloidal pressure) by SICM				Young's modulus $E$ determination using hydrostatic pressure by SICM			Young's modulus $E$ determination by AFM	
	Pipette radius, nm	Ion current, pA	Applied force, nN	Colloidal pressure, Pa	Pipette radius, nm	Ion current, pA	Hydrostatic pressure, Pa	Tip radius, nm	Applied force, nN
Fmoc-FF	57	2500	0,10	4000	205	9020	2000	70	0,25
Acrylamide	50	2200	0,13	16 600	160	7000	9000	70	0,8
Gelatin	50	2200	0,13	10 350	120	5300	40 000	70	2,0

Herein the colloidal pressure for SICM experiment was calculated using formula (5) (see below) with the Fmoc-FF, Acrylamide and Gelatin deformations: 140, 50, 80 nm, correspondingly, that is in agreement with data from Table 1 in the manuscript. The applied pressures for AFM measurements were calculated for the typical deformations for each hydrogel.

#### The calculation of colloidal pressure in the SICM experiments

As it was previously mentioned the intrinsic force  $F$  between pipette and the object was initially obtained on the example of decan drop [Kolmogorov, et.al. 2021, Clarke, et.al. 2016].

Force of surface tension was calculated using the Laplace formula:

$$F_{\sigma} = 2\pi a\sigma \quad (S1)$$

The additional coefficient 2 was used as a radius of the pipette assuming that the whole radius is 2 times bigger than the inner radius of the pipette. So, the force applied by the pipette looks as follows:

$$F = 4\pi\sigma\sqrt{R \cdot d} \quad (S2)$$

where  $\sigma$  is a surface tension parameter. In this experiment the value  $\sigma = 0,25 \cdot 10^{-3}$  N/m [Adewunmi, et.al. 2019].

The colloidal pressure can be estimated as:

$$p = \frac{F}{S} = \frac{F}{\pi a^2} = \frac{F}{\pi R d} \quad (S3)$$

On the example of decan drop the dependence of surface deformation on tip radius was obtained. After that using formula (S2) the dependence of intrinsic force on tip radius was achieved.

In this theory it is assumed that the calibration graph, namely, the dependence of the intrinsic force on the pipette radius, can be used for different samples (cells, soft biomaterials), there is no direct contact between samples and the pipette and the interactions occurs through their double layers.

So, in the experiments with hydrogels the deformation of samples  $d$  was measured using pipette of certain radius  $R$ , after that the colloidal pressure  $p$  was calculated using formula (5), where intrinsic force  $F$  was taken from calibration curve.

- V. S. Kolmogorov, A. S. Erofeev, E. Woodcock, Y. M. Efremov, A. P. Iakovlev, N. A. Savin, A. V. Alova, S. V. Lavrushkina, I. Kireev, A. O. Prelovskaya, E. V. Sviderskaya, D. Scaini, N. L. Klyachko, P. S. Timashev, Y. Takahashi, S. V. Salikhov, Y. N. Parkhomenko, A. G. Majouga, C. R. W. Edwards, P. Novak, Y. E. Korchev, P. V. Gorelkin, *Nanoscale*, 2021, **13**, 6558.
- R. W. Clarke, P. Novak, A. Zhukov, E. J. Tyler, M. Cano-Jaimez, A. Drews, D. Klenerman, *Soft Matter*, 2016, **12**, 7953.
- A. A. Adewunmi, M. S. Kamal, *Energy & Fuels*, 2019, **33**(9), 8456-8462.
- Rico, F., Roca-Cusachs, P., Gavara, N., Farré, R., Rotger, M., & Navajas, D. *Physical Review E—Statistical, Nonlinear, and Soft Matter Physics*, 2005, **72**(2), 021914.

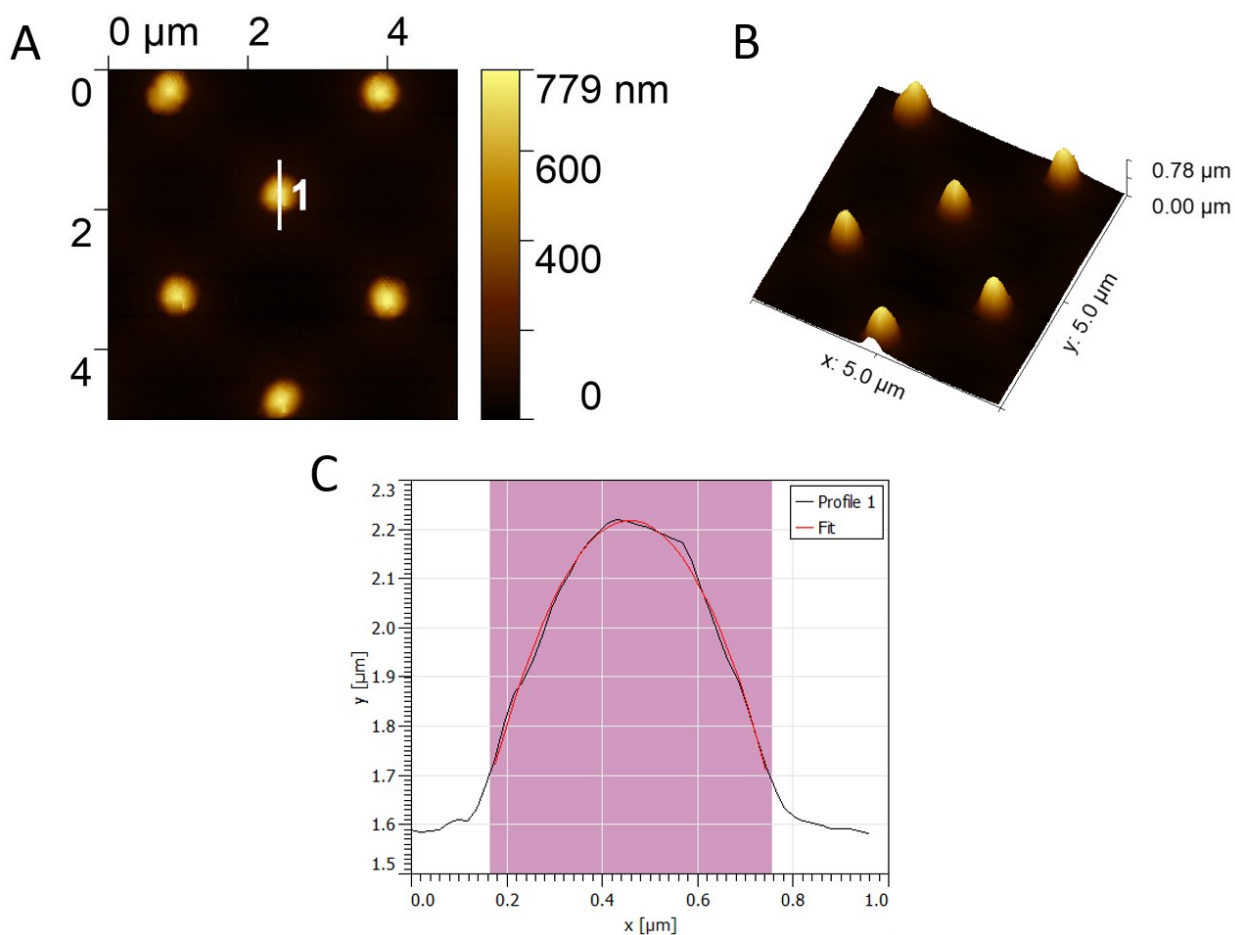


Figure S1. Estimation of the tip shape by scanning the TGT1 calibration grating. (A) Topography of TGT1 calibration grating acquired with the PFQNM-LC-A-CAL probe. (B) 3D representation of the same image. (C) Cross-section over one of the peaks fitted with a quadratic function (red curve).

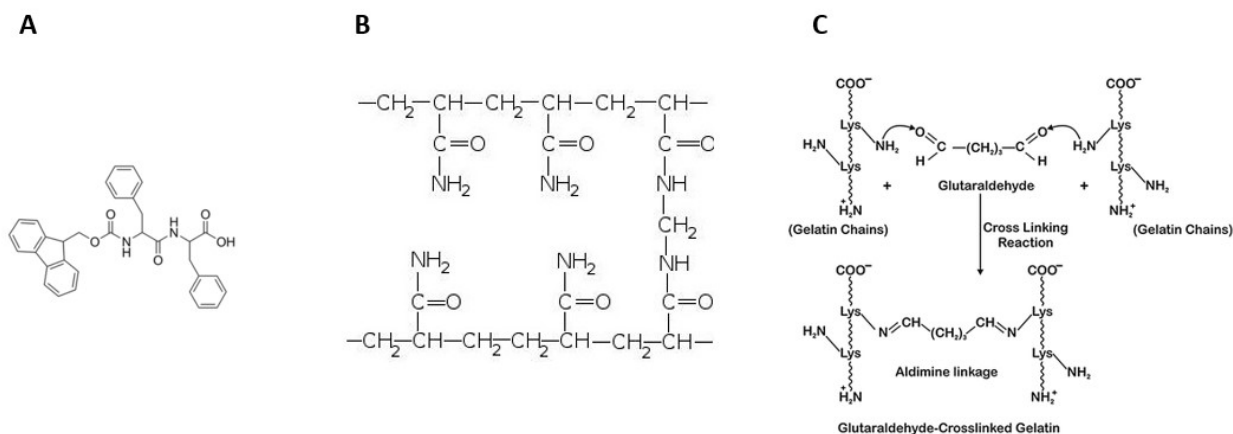


Figure S2. Chemical structures of (A) Fmoc-FF, (B) polyacrylamide and (c) Gelatin (that was crosslinked by glutaraldehyde) hydrogels.

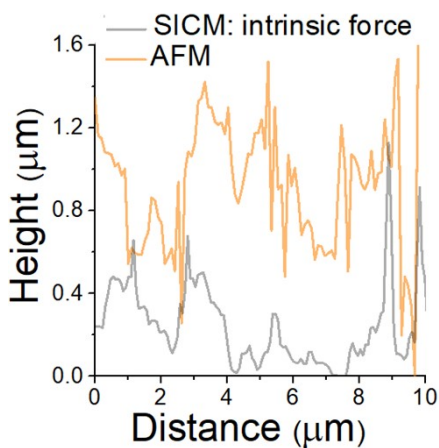


Figure S3. The profile line for Fmoc-FF hydrogel topography image obtained by AFM (orange line) and SICM (grey line)

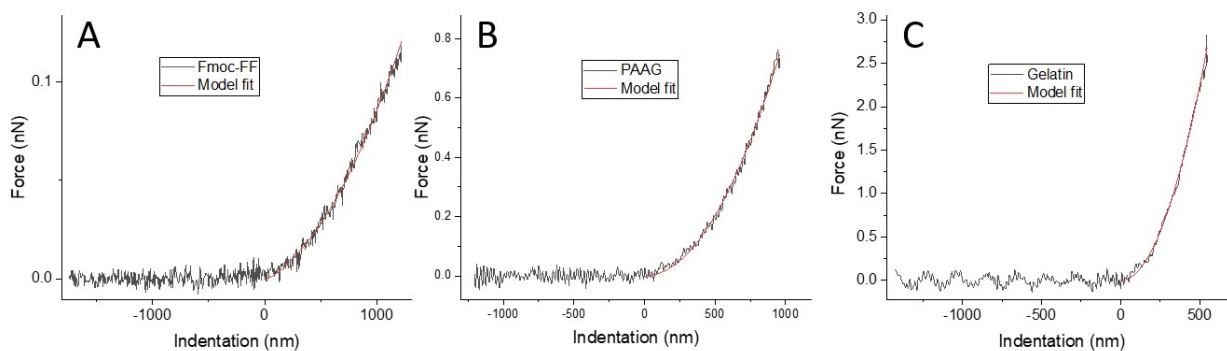


Fig. S4. The force-distance curves for (A) Fmoc-FF, (B) PAAG and (C) Gelatin hydrogels, obtained by AFM.

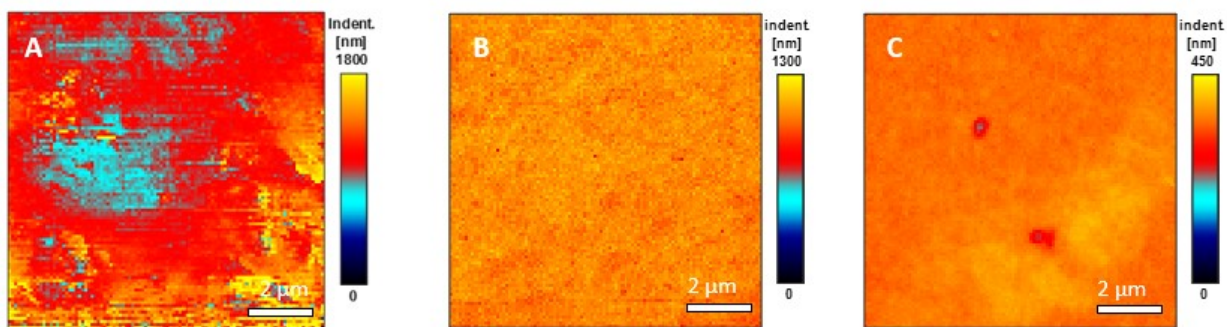


Fig. S5. The indentation maps for (A) Fmoc-FF, (B) PAAG and (C) gelatin hydrogels, obtained by AFM. Scale bar was 2  $\mu\text{m}$ .

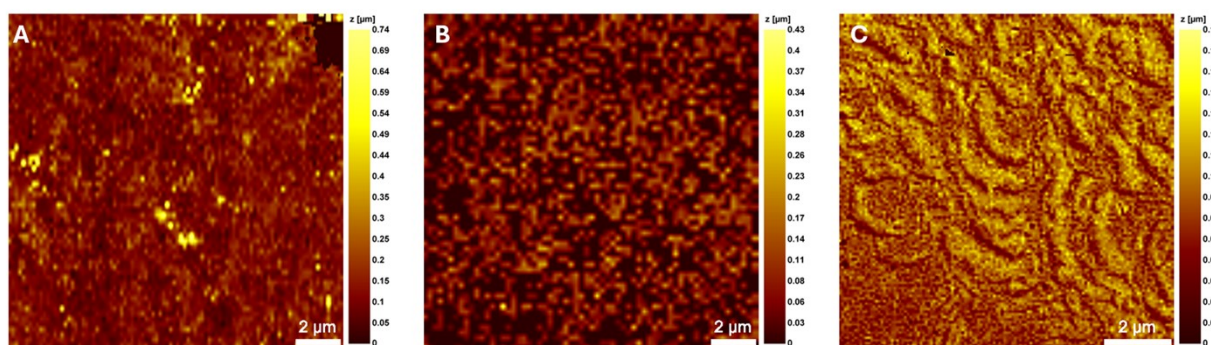


Fig. S6. The indentation maps for (A) Fmoc-FF, (B) PAAG and (C) gelatin hydrogels, obtained by SICM. Scale bar was 2  $\mu\text{m}$ .

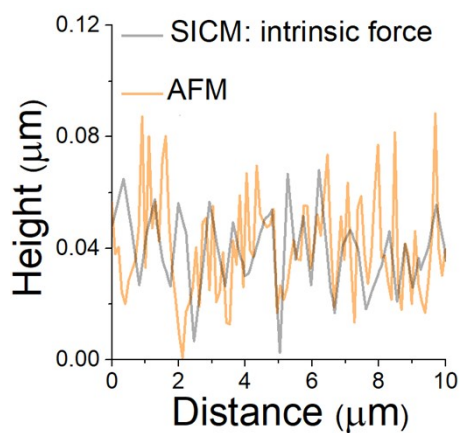


Figure S7. The profile line for polyacrylamide hydrogel topography image obtained by AFM (orange line) and SICM (grey line).

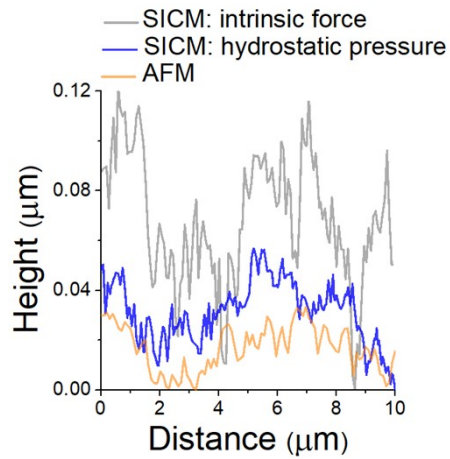


Figure S8. The profile line for gelatin hydrogel topography image obtained by AFM (orange line), SICM using intrinsic force (grey line) and SICM using hydrostatic pressure (blue line).

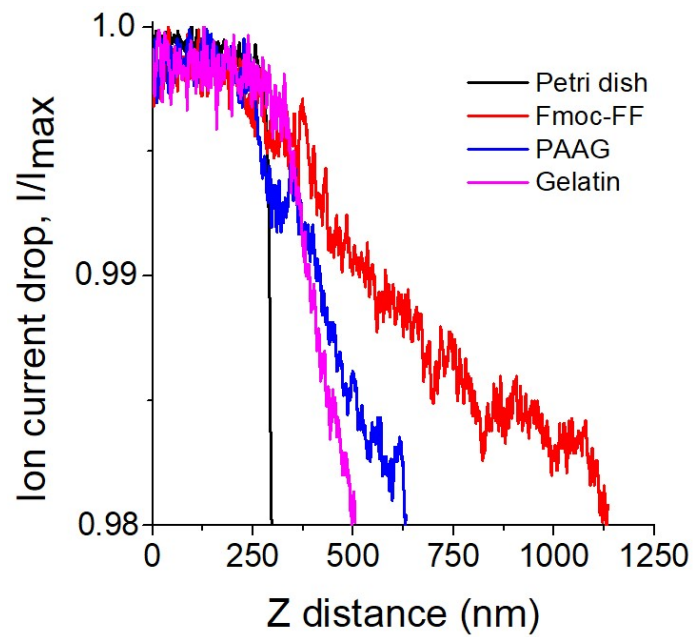


Fig. S9. Ion current-distance curves for SICM method with the application of intrinsic colloidal force for Fmoc-FF, PAAG and gelatin hydrogels.

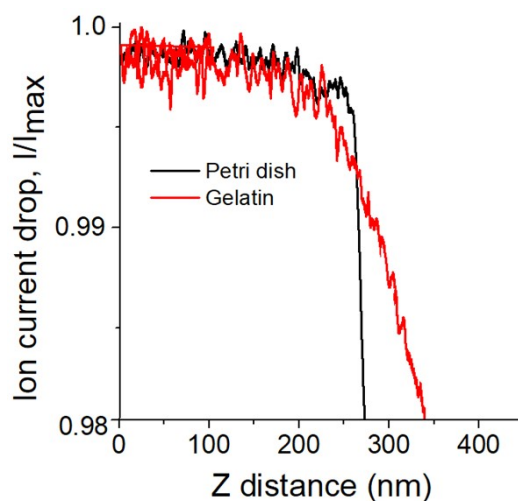


Fig. S10. The current-distance curves, obtained by SICM method with the application of hydrostatic pressure.

Table S2. The comparison between Young's modulus for gels using Hertz and blunted pyramid models.

	Young's modulus (Pa)	
	Blunted pyramid model	Hertz model
<b>Fmoc-FF</b>	350±20	400±20
<b>Polyacrylamide</b>	1700±130	1640±450
<b>Gelatine</b>	17 700±1100	18 020±1340

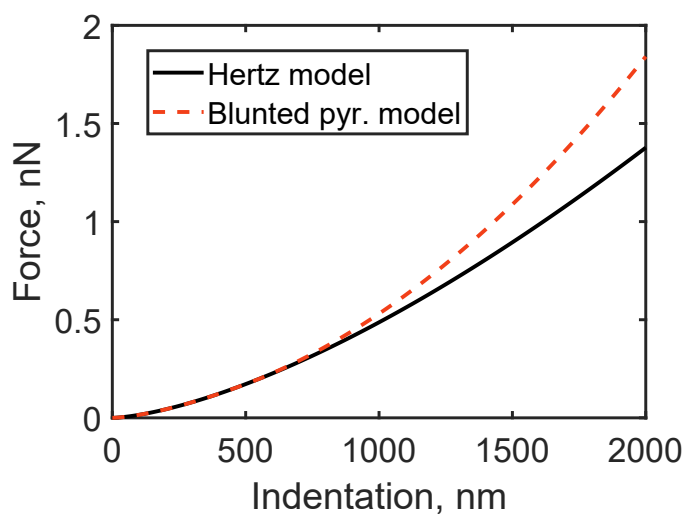


Figure S11. Comparison of the blunted pyramid model and the Hertz's model (for the same arbitrary Young's modulus).

### AFM mechanical measurements with sharp pyramidal probe

Silicon cantilevers with a spring constant of approximately 0.03 N/m and a tip radius of about 10 nm were used (CSC38, MikroMash). The cantilever spring constant was estimated by thermal calibration. Force curves were processed with the contact model for a regular four-sided pyramid (Rico et al., 2005):

$$F = \frac{1}{2^{1/2}} \frac{E \tan \theta}{(1 - \nu^2)} \delta^2 \quad (4)$$

where  $F$  is force,  $E$  is Young's modulus,  $\nu$  is Poisson's ratio,  $\delta$  is indentation, and  $\theta$  is a semi-included angle of a pyramid.

The results acquired with the sharp pyramidal probe are presented in Table S3 and in Fig. S12. The results were consistent between the sharp pyramidal and blunted pyramidal probes, with up to a 10-20% difference in the estimated Young's moduli.

Table S3. The comparison between acquired parameters for gels with blunt and sharp pyramidal probes in AFM experiments.

	Indentation during Young's modulus determination (nm)		Young's modulus (Pa)	
	AFM blunt pyramidal probe	AFM sharp pyramidal probe	AFM blunt pyramidal probe	AFM sharp pyramidal probe
	PFQNM-LC-A-CAL	CSC38	PFQNM-LC-A-CAL	CSC38
<b>Fmoc-FF</b>	1500±50	2500±100	350±20	300 ± 100
<b>Polyacrylamide</b>	950±60	920±20	1700±130	2300± 70
<b>Gelatine</b>	350±15	600±100	17 700±1100	23200± 900



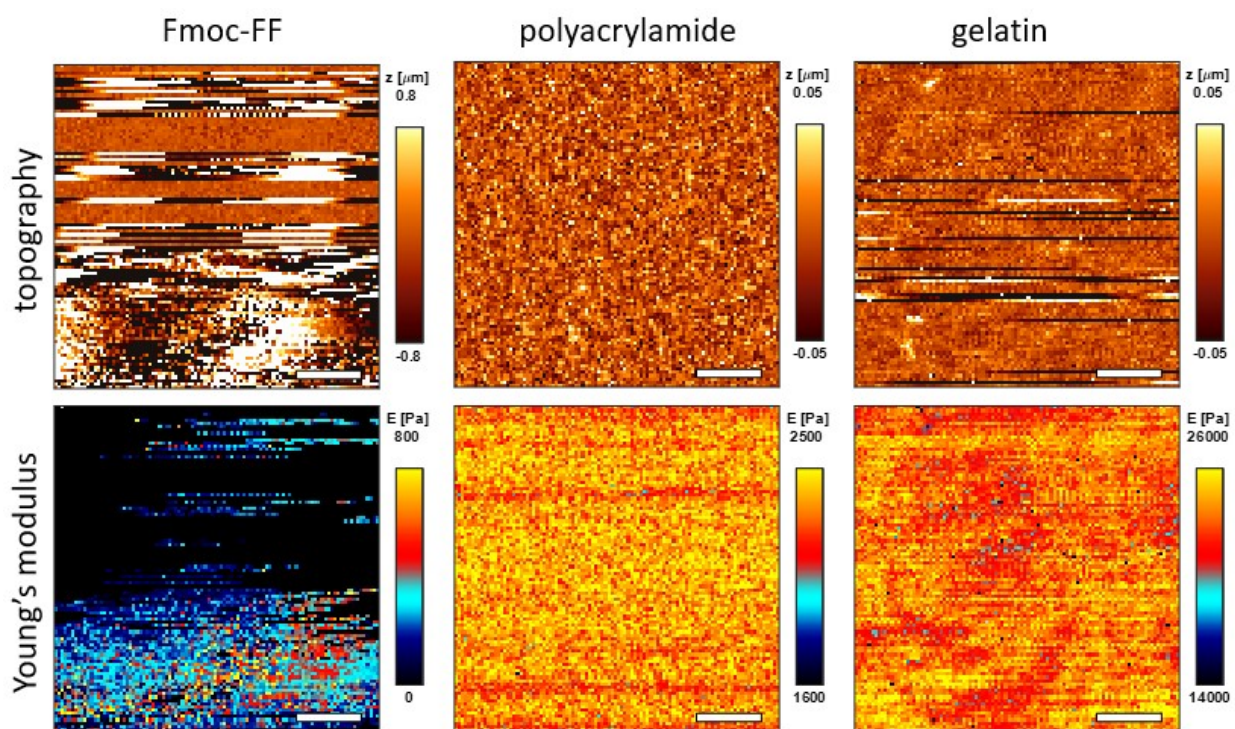


Fig. S12. Image of the hydrogels topography and the mapping of Young's modulus obtained by AFM using sharp pyramidal probe CSC38.